

PNNL-32477

Hot rolling of ZK60 magnesium sheet with isotropic tensile properties from tubing made by Shear Assisted Processing and Extrusion (ShAPE)

December 2021

William E. Frazier
V.V. Joshi
Nicole Overman
Mark Rhodes
Timothy J. Roosendaal
Robert Seffens
Ethan K. Nickerson
Scott Whalen

U.S. DEPARTMENT OF
ENERGY

Prepared for the U.S. Department of Energy
under Contract DE-AC05-76RL01830

DISCLAIMER

This report was prepared as an account of work sponsored by an agency of the United States Government. Neither the United States Government nor any agency thereof, nor Battelle Memorial Institute, nor any of their employees, makes **any warranty, express or implied, or assumes any legal liability or responsibility for the accuracy, completeness, or usefulness of any information, apparatus, product, or process disclosed, or represents that its use would not infringe privately owned rights.** Reference herein to any specific commercial product, process, or service by trade name, trademark, manufacturer, or otherwise does not necessarily constitute or imply its endorsement, recommendation, or favoring by the United States Government or any agency thereof, or Battelle Memorial Institute. The views and opinions of authors expressed herein do not necessarily state or reflect those of the United States Government or any agency thereof.

PACIFIC NORTHWEST NATIONAL LABORATORY
operated by
BATTELLE
for the
UNITED STATES DEPARTMENT OF ENERGY
under Contract DE-AC05-76RL01830

Printed in the United States of America

Available to DOE and DOE contractors from the
Office of Scientific and Technical Information,
P.O. Box 62, Oak Ridge, TN 37831-0062;
ph: (865) 576-8401
fax: (865) 576-5728
email: reports@adonis.osti.gov

Available to the public from the National Technical Information Service
5301 Shawnee Rd., Alexandria, VA 22312
ph: (800) 553-NTIS (6847)
email: orders@ntis.gov <<https://www.ntis.gov/about>>
Online ordering: <http://www.ntis.gov>

Hot rolling of ZK60 magnesium sheet with isotropic tensile properties from tubing made by Shear Assisted Processing and Extrusion (ShAPE)

December 2021

William E. Frazier
V.V. Joshi
Nicole Overman
Mark Rhodes
Timothy J. Roosendaal
Robert Seffens
Ethan K. Nickerson
Scott Whalen

Prepared for
the U.S. Department of Energy
under Contract DE-AC05-76RL01830

Pacific Northwest National Laboratory
Richland, Washington 99354

Abstract

In order to evaluate the viability of ShAPE processed Mg alloys as a feedstock for fabricating lightweight sheet material, tubes consisting of ShAPE-extruded Mg alloy ZK60 were flattened into plates and hot rolled at 450 °C to reductions of 37%, 68%, and 93%. The mechanical properties and microstructure of the rolled material were characterized through tensile testing and electron backscattered diffraction (EBSD). ZK60 specimens rolled to 68% reduction had tensile properties similar to published properties of rolled ZK60 sheets fabricated using conventional processes, and exhibited negligible tensile anisotropy referenced to the rolling direction. Additional rolling from 68% to 93% reduced the ultimate tensile stress in the rolling direction from 341.74 ± 5.96 MPa to 260.76 ± 22.4 MPa. The yield stress and elongation to failure of the material also decreased from 292.16 ± 1.11 MPa to 256.93 ± 18.4 MPa and $6.95 \pm 1.94\%$ to $3.38 \pm 0.51\%$, respectively, but negligible little anisotropy was observed with respect to loading direction. EBSD mapping indicated that the as-extruded ZK60 had texture rotated away from the basal direction which developed into a strong basal texture over numerous hot rolling steps. This evolution in texture has been observed after rolling for hot-rolled ZK60 fabricated through conventional extrusion processes. The initial grain structure was found to have experienced noticeable twinning from flattening the tube into plate. After hot rolling, the grain structure became more equiaxed, but the average grain diameter did not change appreciably from 5.15 ± 3.39 μm in the ShAPE extruded material, to 5.27 ± 12.44 μm in the 93% hot rolled sheet. This response to hot rolling is similar to the response of ZK60 fabricated using other methods such as Equal Channel Angular Processing (ECAP). Therefore, this work demonstrates ShAPE has the potential as an alternative method to producing feedstock for Mg alloy sheets. Modifications to the experimental procedure which could lead to improvements in observed properties are briefly discussed.

Summary

ShAPE-processed ZK60 tubes were mechanically opened and hot-rolled into thin sheets in order to evaluate the quality of the material as rolling feedstock. EBSD evaluation of the tubes indicated that the process of flattening the tubes caused minimal damage to the ZK60 microstructure, but that subsequent hot rolling to 37% and 68% caused the ZK60 texture to rotate back towards a basal texture. The deformation caused by rolling and subsequent recrystallization during reheating of the sheets caused visible changes in the grain structure and the formation of highly strained bands in the sheet that increased in prevalence as reduction increased. However, grain size measurements obtained using EBSD indicated that the grain structure did not appreciably coarsen from the as-ShAPEd grain size. Tensile testing on the 68% and 93% hot-rolled specimens showed that the rolled ZK60 specimens had similar YS, UTS, and ETF to those recorded by other authors for rolled ZK60. Specimens hot rolled to 68% reduction had minimal anisotropy in tensile properties with respect to loading direction, while specimens hot rolled to 93% reduction had some anisotropy. All tested specimens exhibited ductile fracture, but the 93% hot rolled specimens had reduced UTS and ETF. This degradation in mechanical properties has likely occurred due to an accumulation of damage from rolling that had not been dissipated in reheating steps. Therefore, modifications to the rolling and annealing approach used in this work may be able to achieve sheets with improved tensile properties.

Acknowledgments

This work at PNNL was supported by **LDRD TIP Research Info Here**. The authors thank Mark Rhodes and Michael Dahl of PNNL for their assistance and advice in the rolling process. The authors thank Rob Seffens, Timothy Roosendaal, and Ethan Nickerson for their assistance in the tensile testing of specimens. The authors also thank Anthony Guzman for his assistance in sample preparation for microstructural characterization. The authors also acknowledge all the other staff directly or indirectly associated with producing the results featured in this report.

1.0 Introduction

Magnesium alloys are inexpensive to produce and have high strength to weight ratios [1]. However, the properties of Mg alloys, like formability, are generally insufficient for lightweight applications, such as in the automotive industry [2–4]. The weight percentage of magnesium used in a typical passenger car has remained approximately 0.5% for two decades due to these limitations[5,6]. Since the widespread deployment of Mg alloys in the automotive industry could lead to significant improvements in vehicle fuel efficiency, Mg alloy formability has been the subject of considerable research interest.

Mg alloys have low formability at room temperature [3,7,8], although recent experimental work has shown that it is possible to process pure Mg for high formability at room temperature [9]. The reason for this typically low formability is that Mg alloys have a hexagonal close packed (HCP) crystal structure and greatly prefers basal slip when deformed at room temperature [10–13]. However, in order to accommodate plastic deformation, five different slip systems (in addition to twinning) must be active to meet the von mises criterion [14]. This is a considerable technical obstacle, as prismatic $\langle a \rangle$, pyramidal $\langle a \rangle$, and pyramidal $\langle a+c \rangle$ slip all have critical resolved shear stresses multiple times higher than basal $\langle a \rangle$ slip [13]. Numerous strategies exist in order to circumvent or alleviate this limitation. For example, the addition of rare earth (RE) elements to Mg alloys roughens the slip planes, making additional modes of deformation achievable [15–17] and has the further effect of refining the grain structure, promoting grain boundary sliding [17–19]. This improves alloy formability, but the additive REs required are expensive [4]. Forming at temperatures between 280 °C and 500 °C generally improves alloy deformation response [11,20], but is an energy intensive process. Twin-roll casting, for example, is a common method used to fabricate Mg alloys [21]. Other authors have attempted to form Mg alloys using multiple cold rolling and annealing steps, such as Zhang *et al.*, who were recently able to achieve refined grain structure and formability in AZ31 through repeated 10-15% cold rolling passes with 30 minute intermediate anneals at 250 °C [16]. Such a process is energy intensive and time intensive due to the required annealing periods.

Different extrusion techniques that cause severe plastic deformation (SPD) have been the subject of recent interest due to their potential to refine the Mg grain structure, which promotes grain boundary sliding during deformation [17,19]. One of these techniques, equal channel angular processing (ECAP), is also capable of rotating Mg texture away from the basal texture after multiple passes [12,22]. This process has been able to improve the yield strength, formability, and extension to failure of Mg alloys [12,22–24] and even hydrogen storage properties [25]. Unfortunately, the batch size and scalability of this and most other SPD methods are currently limited to amounts that would not be feasible for industrial level production [5]. However, a new form of friction stir back extrusion (FSBE) called Shear Assisted Processing and Extrusion (ShAPE) has recently shown promise as a method to control Mg alloy grain size and texture [5,26–29]. ShAPE has several primary advantages over other existing SPD methods. First, unlike ECAP and other methods, ShAPE is able to produce long hollow-section extrusions, which is necessary for application in certain structure components [5]. Second, ShAPE is able to produce extrusions with large outer diameters and high extrusion ratios in comparison to other FSBE methods, giving it promise as a scalable method. Finally, ShAPE is able to produce extrusions with wall thicknesses of less than a millimeter [26], which means that it could potentially be fabricated and then formed into a sheet with minimal rolling. Previous work that explored the properties and

microstructure of ShAPE extruded ZK60 report that the alloy had an ultimate tensile strength between 250 and 300 MPa, with 20-25% extension to failure [29].

It has yet to be published in literature whether or not ShAPE extruded ZK60 retains its microstructure and mechanical properties when formed from a tube into a plate and subsequently rolled. This information would be particularly useful in order to evaluate the viability of ShAPE extruded ZK60 as rolling feedstock, and to inform ShAPE processing parameters. Therefore, the goal of this work is to characterize a rolled ZK60 microstructure and quantify its mechanical properties.

2.0 Experimental Methods

Extruded ZK60 tubes were fabricated from ZK60-T5 bar and as-cast billets using the method described by Whalen et al [5]. This resulted in tubes having an outer diameter of 50.8 mm and wall thickness of 1.9 mm which were then sectioned into approximately 200 mm long sections. After sectioning, the tubes were cut along the extrusion direction and forced open at room temperature using a vice. A schematic diagram of the process of opening and rolling the ShAPE-fabricated tubes is shown in Fig. 1.

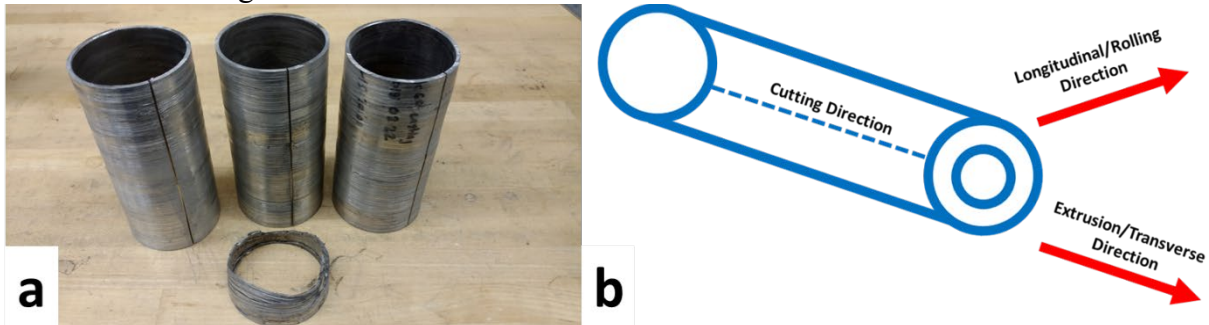


Fig 1. Three ShAPE-processed ZK60 tubes before being opened for rolling (a). A schematic diagram of the extruded ZK60 tubes, showing the extrusion direction of the tubes with respect to the rolling direction of the flattened plates (b).

The flattened plates were then heated in air at 450 °C for periods of five minutes using a standard furnace, and then immediately cold-rolled. In order to minimize heat loss, the plates were moved from the furnace to the rollers on a hot plate. Each rolling pass had a targeted reduction of approximately 15%. The 1.9 mm tubes were flattened and rolled until a final thickness 1.3 mm, 0.64 mm, and 0.13 mm correspond to total reductions of 37%, 68%, and 93%, respectively. Of these, the samples with 37% reduction and 68% reduction were examined using electron backscattered diffraction (EBSD). These levels of reduction were selected because above this level of reduction patterns became difficult to capture in EBSD. For the purpose of comparison, a sample obtained from the flattened tube, prior to rolling, was also examined using EBSD. Prior to microstructural analysis, specimens were mounted in epoxy and polished to a final surface finish of 0.05 μm using colloidal silica. Scanning electron microscopy (SEM) analysis was performed using a JEOL 7600F field emission scanning electron microscope. Electron backscatter diffraction (EBSD) mapping was performed using an accelerating voltage of 20keV and a working distance of ~24mm. Indexing was accomplished using a magnesium hexagonal crystal structure, Laue group 9, space group 194 and unit cell parameters $a=3.209\text{\AA}$, $b=3.209\text{\AA}$, $c=5.211\text{\AA}$, $\alpha=90^\circ$, $\beta=90^\circ$, $\gamma=120^\circ$. It should be noted that only the matrix phase was mapped for EBSD analysis. Refined second phase precipitates were not included in the EBSD analysis, due to the large length scales that the texture evaluation was performed across. From this microscopy, the grain structure of the samples through the thickness was determined, using cross sections cut in both the rolling and transverse directions. Pole figures of the grain orientations were also obtained in order to determine any changes in texture.

Mechanical testing of ZK60 specimens was performed using ASTM E8 on a 5k servo hydraulic load frame using hydraulic knurled wedge grips. The 68% hot rolled specimens were cut into

tensile specimens 29.2 mm long, 6.38 mm wide, and 0.571 mm thick, while the 93% hot rolled samples were cut into tensile specimens 21.9 mm long, 4.85 mm wide, and 0.157 mm thick. Digital image correlation (DIC) was used in order to determine extension with respect to loading. The samples with 68% reduction and 93% reduction were cut into tensile testing specimens oriented in the rolling, transverse, and at a 45° angle from the rolling direction. This testing allowed us to establish the effect of additional rolling treatment on mechanical performance and anisotropy. Three tensile tests were performed for each specimen thickness and orientation, and from these tests the 0.02% yield stress, ultimate tensile stress, and % elongation to failure were determined. The fractured surfaces on each tensile specimen were photographed in order to diagnose the type of failure that occurred. These results in comparison to the measurements on as-extruded ZK60 from Whalen *et al.* [5,29] helped us to ascertain the extent to which ShAPE processed ZK60 retains texture, grain structure, and mechanical properties from the as-extruded tube.

3.0 Results

Longitudinal, through-thickness sections of the ZK60 samples for the ShAPE extruded and flattened, 37% hot rolled, and 68% hot rolled sheets are shown in Fig. 2. In the ShAPE extruded and flattened microstructure, it is observed that the grain structure is close to equiaxed. The inverse pole figures of the microstructure show that twinning has apparently occurred during the flattening process (please note the thumbnail in Fig. 2), which was done at room temperature. However, the microstructure appears to have maintained the majority of its texture and uniformity from Whalen *et al.* [5].

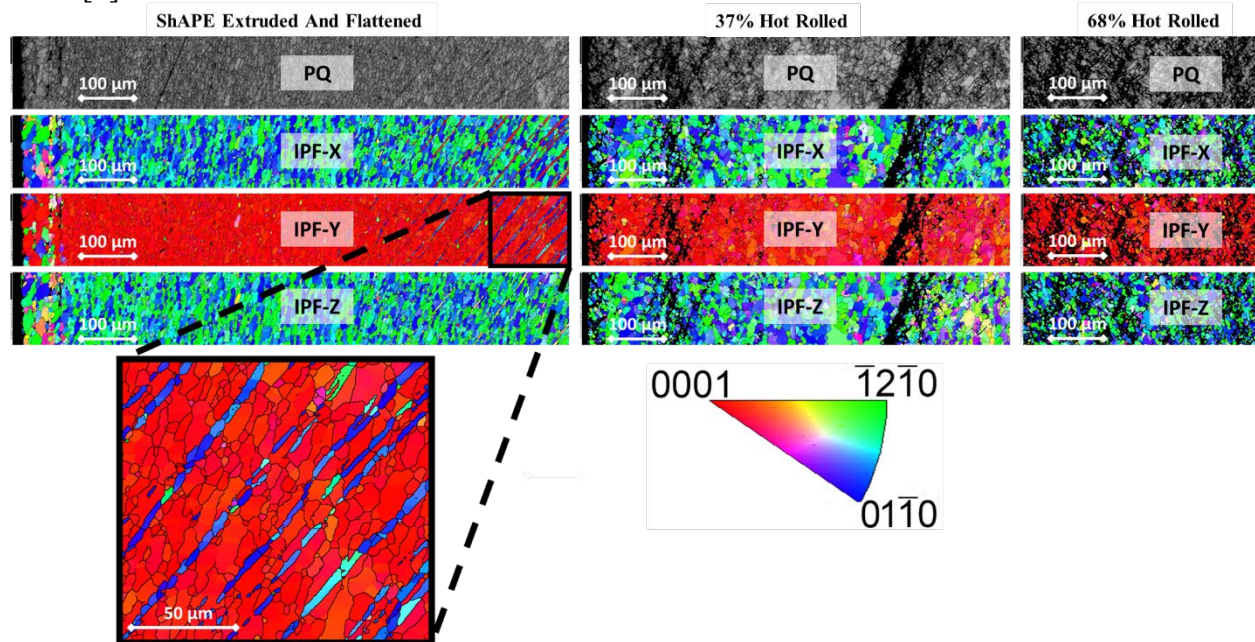


Figure 2. Through-thickness EBSD maps of the ShAPE extruded and flattened, 37% hot rolled, and 68% hot rolled ZK60 specimens in the longitudinal section. In each map, the left side is the outer diameter of the tube, while the right side is the inner diameter of the tube.

The only sign of deformation in the as-flattened microstructure appears to be the twinning observed in EBSD, with no obvious signs of accumulated dislocation density or other adverse effects. Deformation twinning in Mg alloys has been previously reported by numerous authors [30,31]. Deformation twins are thought to increase strength and ductility in metals by acting as additional obstacles to dislocation motion [31]. A measurement of the misorientation profile between the apparent twinned grains from Fig. 4 confirms that these grains are twins, shown in Fig. 3.

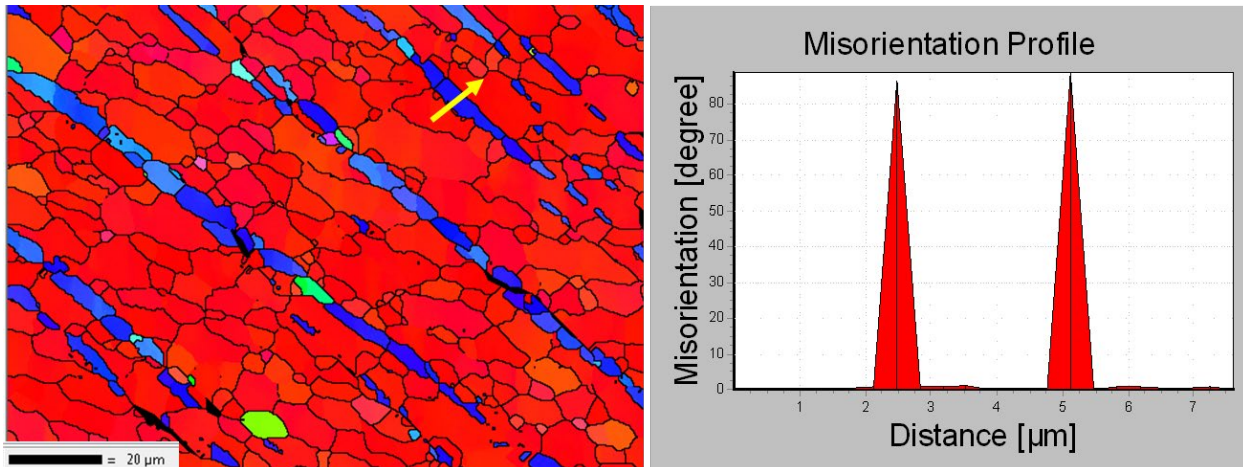


Figure 3. The deformation twinning between two grains in the as-flattened ZK60, demonstrated by a misorientation profile on an EBSD map of the as-flattened ZK60 plate.

When plotted to show orientation density, it is observed that the microstructure is slightly rotated away from the basal texture, Fig. 4. With the applied hot rolling and reheating treatment, the texture visibly rotates towards the basal texture in each successive reduction, with the 68% reduction being rotated almost entirely to a basal texture. The through-thickness scans of the sheets show that while the as-flattened sheet has a very uniform microstructure, after 37% reduction there are grains that have visibly grown and deviated from the as-extruded texture. Bands have also appeared in which EBSD was unable to determine a grain orientation, which either indicates that the region has been highly deformed or that the region has very fine recrystallized grains. After 68% reduction, more grains have visibly grown, although the variations from the initial texture are still relatively small. However, the bands in which EBSD was unable to determine a pattern consisted of a larger fraction of the microstructure.

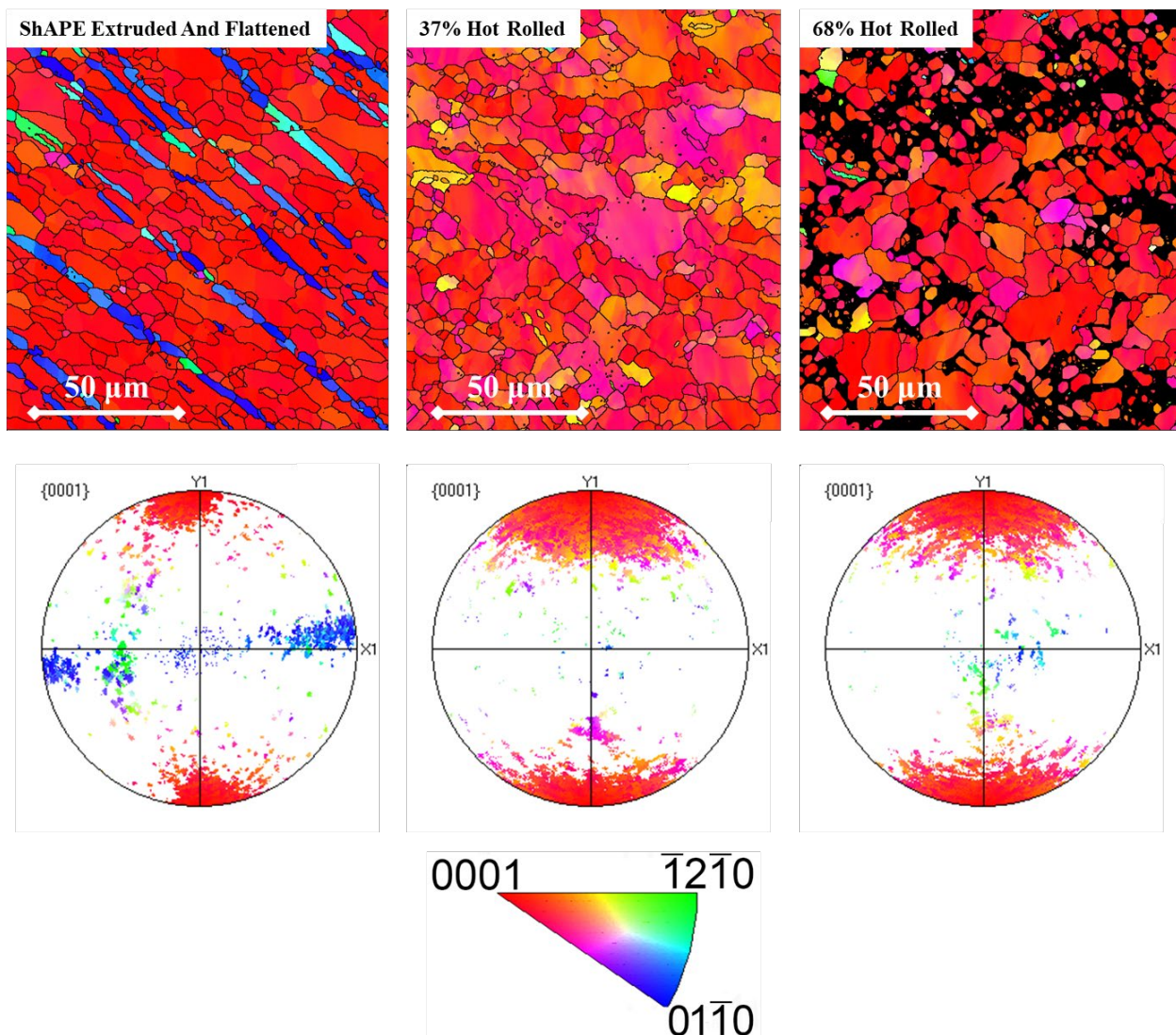


Figure 4. EBSD maps and pole figures of the ShAPE extruded and flattened, 37% hot rolled, and 68% hot rolled ZK60 specimens in the longitudinal section.

A similar trend can be seen for transverse sections of the ZK60 samples, as shown in Fig. 5. These results also indicate that despite the initial rotation away from the basal texture as a result of the ShAPE process, the multiple rolling passes cause rotation back towards the basal texture.

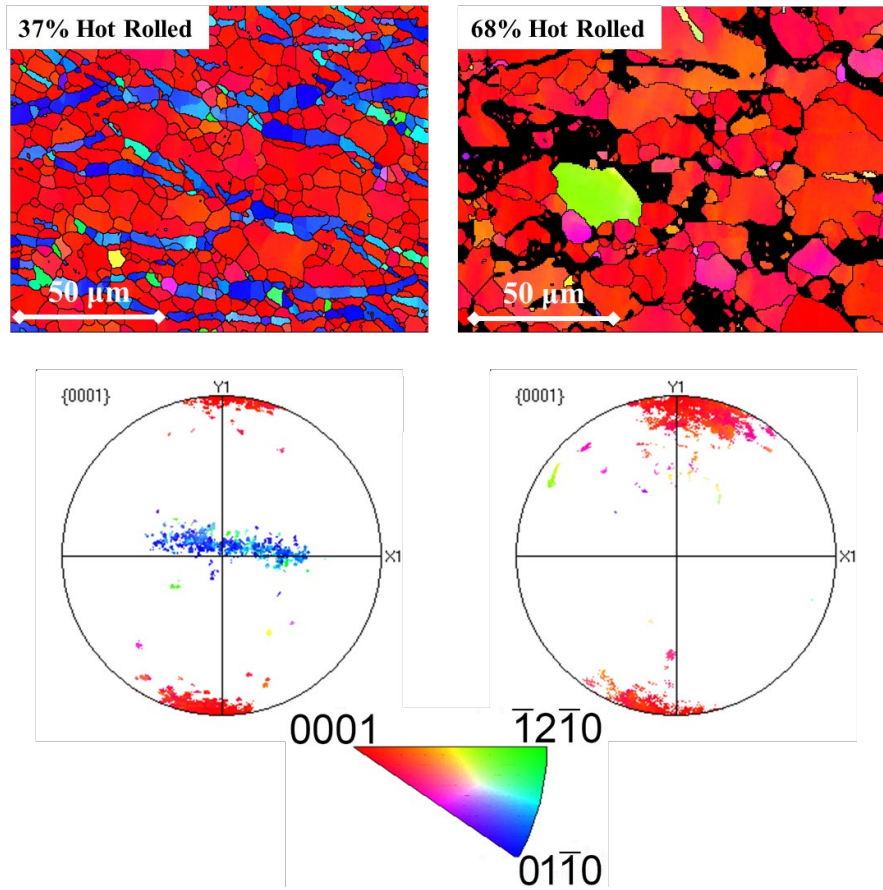


Figure 5. EBSD maps and pole figures of the ShAPE extruded, 37% hot rolled, and 68% hot rolled ZK60 specimens in the transverse section.

45Plots of the grain size distribution for each scanned microstructure, taken from longitudinal sections, indicate relatively small changes in average grain diameter, shown in Fig. 6. Although the rolling process has visibly changed the grain structure, the average grain size remains approximately the same, beginning at $5.15 \pm 3.39 \mu\text{m}$ in the ShAPE extruded material, and $5.27 \pm 3.53 \mu\text{m}$. Notably, this excludes the regions of the rolled specimens where obtaining a pattern was not possible. If these grains were either very fine due to recrystallization or simply highly deformed large grains, this estimate could have considerable error, so those regions were not considered in the grain size analysis. It is also noticeable that while the average grain diameter only slightly increases with rolling treatment, the maximum grain size after hot rolling has increased considerably.

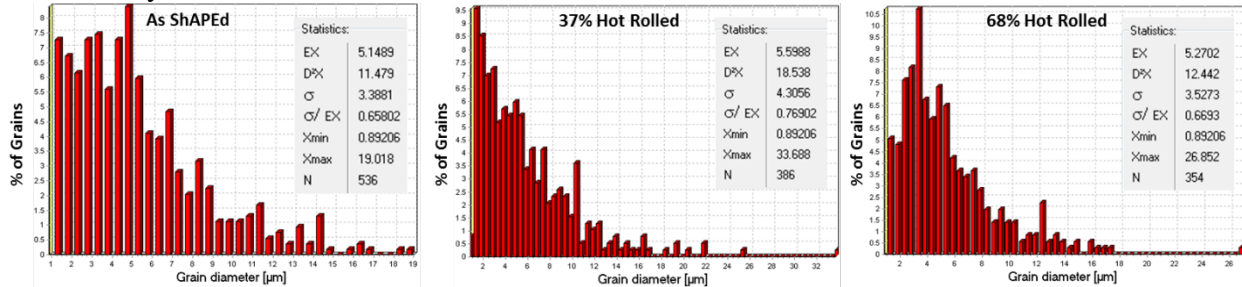


Figure 6. The grain size distributions of ShAPE extruded, 37% hot-rolled, and 68% hot-rolled ZK60 specimens, as taken from EBSD scans on longitudinal sections.

Tensile properties of the rolled specimens indicate that rolling at first creates an increase in strength at the expense of elongation to failure. Plots of tensile behavior for 68% rolled specimens in the rolling direction, transverse direction, and 45° to rolling show that ultimate tensile stress (UTS) reaches over 330 MPa in each case, as shown in Fig. 7a-c. This is a significant increase from the measured UTS by Whalen *et al.* [29]. However, most of the specimens do not reach 10% extension to failure, which is a significant decrease from Whalen's observations. This behavior is not surprising, as other experimental efforts to form magnesium alloys have also reported increased strength and reduced elongation to failure, even after the use of extrusion processes to refine grain structure and improve texture [12]. It is notable that Whalen *et al.* reported noticeable anisotropy between the UTS of the rolling, transverse, and 45° tensile specimens, over 40 MPa, while our specimens have less than 10 MPa of variation. This suggests that hot rolling at this point has reduced the tensile anisotropy of the material.

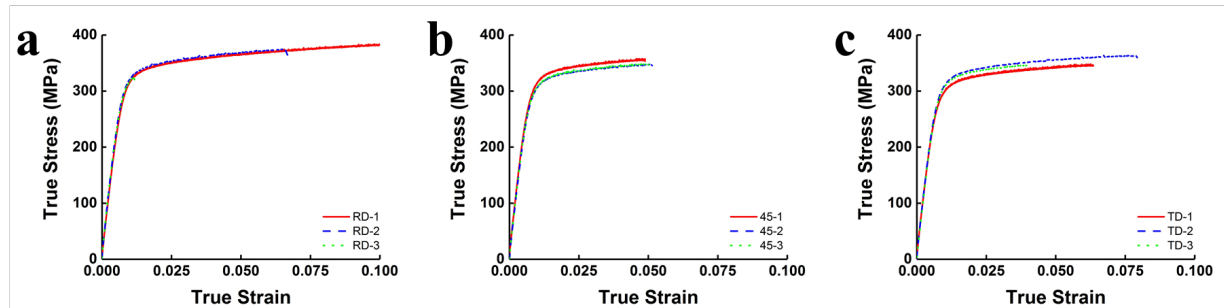


Figure 7. The tensile stress-strain curves of the ShAPE-processed ZK60 flattened and hot rolled to 68% reduction. Plots are shown for loading in the rolling direction (a), 45° to the rolling direction (b), and the transverse direction (c).

Additional rolling appears to lead to an overall reduction in tensile properties and an increase in the apparent anisotropy, however. The 93% rolled specimens, regardless of direction, all have an average UTS of less than 300 MPa and even smaller elongation to failure (ETF) than the 68% rolled specimens. Considerably more variation in the mechanical behavior is noticeable. The variation in UTS with tensile direction at the same time has increased to nearly 25 MPa. This is still less variation than that observed for the ShAPE extruded material. The plots of these tensile stress-strain curves are shown in Fig. 8a-c. The average yield stress, UTS, and ETF for the 68% and 93% rolled specimens is shown in Table 1.

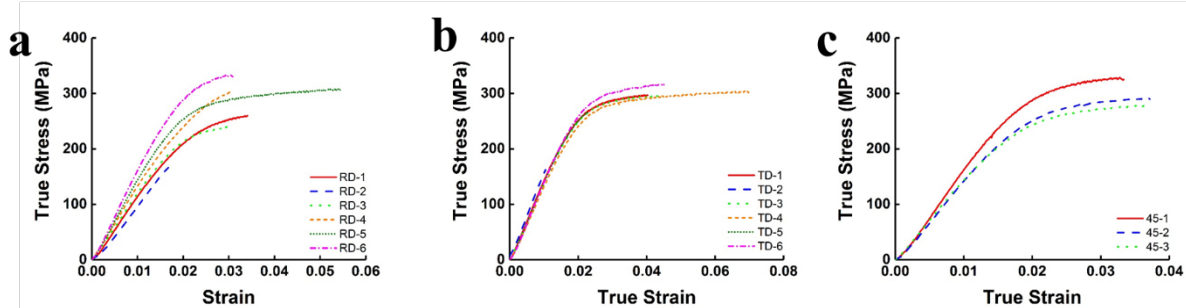


Figure 8. The tensile stress-strain curves of the ShAPE-processed ZK60 flattened and hot rolled to 93% reduction. Plots are shown for loading in the rolling direction (a), 45° to the rolling direction (b), and the transverse direction (c).

Table 1. The tensile properties of ShAPE-processed ZK60 after hot rolling.

Direction	68% Reduction			93% Reduction		
	YS (MPa)	UTS (MPa)	ETF %	YS (MPa)	UTS (MPa)	ETF %
RD	292.16±1.11	341.74±5.96	6.95±1.94	256.93±18.4	260.76±22.4	3.38±0.51
TD	286.19±1.13	336.09±1.58	5.15±0.05	251.91±18.9	262.83±21.2	4.00±0.87
45°	284.33±3.18	334.61±2.12	6.31±0.71	272.81±19.1	289.28±14.8	3.64±0.12

It is important to mention, for example, that while the ZK60 sheets in this work were rolled immediately after heating, the sheets were not held at an elevated temperature for rolling, and the rollers themselves were not heated. A hot plate was used to mitigate heat loss in the Mg sheet during transfer to the rolling mill, but it is conceivable that this cooling causes the sheet to experience significant cold work, especially as the sheet decreases in thickness and cools more rapidly. Therefore, the repetition of this work using a hot rolling mill could foreseeably improve sheet properties. As a demonstration of this, the UTS and YS results for transverse direction samples on Table 1 are plotted next to results on tests from the other side of the sheet, which entered the roller last, in Table 2.

Table 2. The tensile properties of ShAPE-processed ZK60 after 93% reduction by hot rolling, as affected by the position of the sample on the rolled sheet.

Orientation	YS (MPa)	UTS (MPa)	ETF %
TD - Front	272.15±10.5	282.37±12.5	4.72±1.42
TD - Back	231.67±35.6	243.29±41.4	3.28±1.12

Examination of the fractured specimens shows that the fracture occurred at an approximately 45° angle with respect to the loading axis in all specimens, regardless of the orientation of the sample or its rolled thickness. Photographs of specimens from the 68% reduction in each orientation are shown as an example in Fig 9. This behavior is consistent with failure by ductile fracture as is observed to be similar across all reductions.

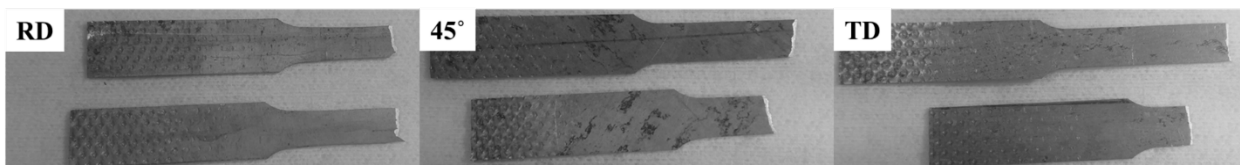


Figure 9. Fractured tensile specimens from 68% hot-rolled ZK60, loaded in the rolling direction (RD), 45° to the rolling direction (45°), and transverse direction (TD).

4.0 Discussion

However, the ShAPE-fabricated tubes must also retain their properties through flattening and additional forming steps for feasible use as rolling feedstock. This work has demonstrated that the ShAPE extruded tubes can feasibly survive the process of forming into plates with minimal accumulation of damage.

This work has also established that it is possible to hot roll ShAPE extruded ZK60 to the thicknesses required for industrial applications. The tensile properties reported are comparable with those obtained through the use of other processes, given the amount of mechanical work applied the material. However, modifications to the rolling schedule used in this work may lead to significant improvements over the measured properties.

The rolling temperature, annealing treatment, and reduction per pass may also foreseeably improve sheet performance. Previous experimentation on hot-pressed ZK 60 by Wang *et al.* has shown that at annealing temperatures of 400 °C, recrystallization occurred in under 1,000 seconds, and in the same time the grain structure coarsened from roughly 2 µm to 7 µm [10]. This suggests that the time taken to reheat in this work, five minutes (300 seconds) at 450 °C, should have been sufficient to cause significant static recrystallization, but may not have been enough to entirely recrystallize the material. The work by Wang, amongst others [11,18,32,33], has reported the formation of highly strained bands within the deformed grain structure after rolling, which is similar to our observation in this work for 37% and 68% rolled specimens. It is notable that Wang *et al.* reports that at 1,000 seconds at 400 °C, the grain structure was completely recrystallized, but that 5,000 seconds of annealing at temperature were required to cause the microstructure to become equiaxed [10]. If the performance of the sheet were affected by this change in the grain structure, then additional annealing may significantly improve tensile properties and rollability for subsequent passes. Jin *et al.*, for example, was able to greatly improve the elongation to failure of ZK60 hot rolled to 63% reduction in thickness by using an electropulsing treatment [34]. This also suggests that the tensile properties of the rolled ZK60 in this work may be greatly improved by a final anneal.

5.0 References

1. B.L. Mordike, T. Ebert, Magnesium Properties - applications - potential, *Mater. Sci. Eng. A.* 302 (2001) 37–45. doi:10.1016/S0921-5093(00)01351-4.
2. E. Aghion, B. Bronfin, D. Eliezer, The role of the magnesium industry in protecting the environment, *J. Mater. Process. Technol.* 117 (2001) 381–385. doi:10.1016/S0924-0136(01)00779-8.
3. J. Hirsch, T. Al-Samman, Superior light metals by texture engineering: Optimized aluminum and magnesium alloys for automotive applications, *Acta Mater.* 61 (2013) 818–843. doi:10.1016/j.actamat.2012.10.044.
4. W.J. Joost, P.E. Krajewski, Towards magnesium alloys for high-volume automotive applications, *Scr. Mater.* 128 (2017) 107–112. doi:10.1016/j.scriptamat.2016.07.035.
5. S. Whalen, N. Overman, V. Joshi, T. Varga, D. Gra, C. Lavender, Magnesium alloy ZK60 tubing made by Shear Assisted Processing and Extrusion (ShAPE), *Mater. Sci. Eng. A.* 755 (2019) 278–288. doi:10.1016/j.msea.2019.04.013.
6. Lightweight Materials R&D: FY14 Annual Progress Report, 2015.
7. M.Z. Bian, T.T. Sasaki, T. Nakata, S. Kamado, K. Hono, Effects of rolling conditions on the microstructure and mechanical properties in a Mg – Al – Ca – Mn – Zn alloy sheet, *Mater. Sci. Eng. A.* 730 (2018) 147–154. doi:10.1016/j.msea.2018.05.065.
8. B.C. Suh, M.S. Shim, K.S. Shin, N.J. Kim, Current issues in magnesium sheet alloys: Where do we go from here?, *Scr. Mater.* 84–85 (2014) 1–6. doi:10.1016/j.scriptamat.2014.04.017.
9. Z. Zeng, J.F. Nie, S.W. Xu, C.H.J. Davies, N. Birbilis, Super-formable pure magnesium at room temperature, *Nat. Commun.* 8 (2017) 1–5. doi:10.1038/s41467-017-01330-9.
10. S. Wang, S.B. Kang, J. Cho, Effect of hot compression and annealing on microstructure evolution of ZK60 magnesium alloys, *J. Mater. Sci.* 44 (2009) 5475–5484. doi:10.1007/s10853-009-3762-7.
11. W. Wang, W. Chen, W. Zhang, G. Cui, E. Wang, Effect of deformation temperature on texture and mechanical properties of ZK60 magnesium alloy sheet rolled by multi-pass lowered-temperature rolling, Elsevier B.V., 2018. doi:10.1016/j.msea.2017.12.024.
12. Y. Yuan, A. Ma, X. Gou, J. Jiang, F. Lu, D. Song, Y. Zhu, Superior mechanical properties of ZK60 mg alloy processed by equal channel angular pressing and rolling, Elsevier, 2015. doi:10.1016/j.msea.2015.02.004.
13. A. Styczynski, C. Hartig, J. Bohlen, D. Letzig, Cold rolling textures in AZ31 wrought magnesium alloy, 2004. doi:10.1016/j.scriptamat.2004.01.010.

14. T. G I, Plastic strain in metals, *J. Inst. Met.* 62 (1938) 307–324.
15. M. Jahedi, B.A. McWilliams, M. Knezevic, Deformation and fracture mechanisms in WE43 magnesium-rare earth alloy fabricated by direct-chill casting and rolling, *Mater. Sci. Eng. A.* 726 (2018) 194–207. doi:10.1016/j.msea.2018.04.090.
16. H. Zhang, W. Cheng, J. Fan, B. Xu, H. Dong, Improved mechanical properties of AZ31 magnesium alloy sheets by repeated cold rolling and annealing using a small pass reduction, *Mater. Sci. Eng. A.* 637 (2015) 243–250. doi:10.1016/j.msea.2015.04.057.
17. H. Somekawa, A. Singh, T. Mukai, T. Inoue, Effect of alloying elements on room temperature tensile ductility in magnesium alloys, Elsevier B.V., 2016. doi:10.1080/14786435.2016.1212174.
18. H. Guo, X. Zeng, J. Fan, H. Zhang, Q. Zhang, W. Li, H. Dong, B. Xu, Effect of electropulsing treatment on static recrystallization behavior of cold-rolled magnesium alloy ZK60 with different reductions, *J. Mater. Sci. Technol.* 35 (2019) 1113–1120. doi:10.1016/j.jmst.2018.11.008.
19. Y.H. Wei, Q.D. Wang, Y.P. Zhu, H.T. Zhou, W.J. Ding, Y. Chino, M. Mabuchi, Superplasticity and grain boundary sliding in rolled AZ91 magnesium alloy at high strain rates, *Mater. Sci. Eng. A.* 360 (2003) 107–115. doi:10.1016/S0921-5093(03)00407-6.
20. D. Nugmanov, M. Knezevic, M. Zecevic, O. Situdikov, M. Markushev, I.J. Beyerlein, Origin of plastic anisotropy in (ultra)-fine-grained Mg–Zn–Zr alloy processed by isothermal multi-step forging and rolling: Experiments and modeling, Elsevier B.V., 2018. doi:10.1016/j.msea.2017.12.045.
21. J.H. Cho, S.S. Jeong, S.B. Kang, Deep drawing of ZK60 magnesium sheets fabricated using ingot and twin-roll casting methods, *Mater. Des.* 110 (2016) 214–224. doi:10.1016/j.matdes.2016.07.131.
22. C. Wang, A. Ma, J. Sun, H. Liu, H. Huang, Z. Yang, Effect of ECAP process on as-cast and as-homogenized Mg-Al-Ca-Mn alloys with different Mg₂Ca morphologies, *J. Alloys Compd.* 793 (2019) 259–270. doi:10.1016/j.jallcom.2019.04.202.
23. S.R. Agnew, J.A. Horton, T.M. Lillo, D.W. Brown, Enhanced ductility in strongly textured magnesium produced by equal channel angular processing, 2004. doi:10.1016/j.scriptamat.2003.10.006.
24. J. Suh, J. Victoria-Hernandez, D. Letzig, R. Golle, S. Yi, J. Bohlen, W. Volk, Improvement in cold formability of AZ31 magnesium alloy sheets processed by equal channel angular pressing, 2014. doi:10.1016/j.jmatprotec.2014.11.029.
25. M. Krystian, M.J. Zehetbauer, H. Kropik, B. Mingler, G. Krexner, Hydrogen storage properties of bulk nanostructured ZK60 Mg alloy processed by Equal Channel Angular Pressing, Elsevier B.V., 2011. doi:10.1016/j.jallcom.2011.01.029.

26. N.R. Overman, S.A. Whalen, M.E. Bowden, M.J. Olszta, K. Kruska, T. Clark, E.L. Stevens, J.T. Darsell, V. V. Joshi, X. Jiang, K.F. Mattlin, S.N. Mathaudhu, Homogenization and texture development in rapidly solidified AZ91E consolidated by Shear Assisted Processing and Extrusion (ShAPE), Elsevier B.V., 2017. doi:10.1016/j.msea.2017.06.062.

27. J.T. Darsell, N.R. Overman, V. V Joshi, S.A. Whalen, S.N. Mathaudhu, Shear Assisted Processing and Extrusion (ShAPE) of AZ91E Flake : A Study of Tooling Features and Processing Effects, *J. Mater. Eng. Perform.* 27 (2018) 4150–4161. doi:10.1007/s11665-018-3509-1.

28. M. Jamalian, V. V Joshi, S. Whalen, C. Lavender, D.P. Field, Microstructure and Texture Evolution of Magnesium alloy after Shear Assisted Processing and Extrusion (ShAPE TM) Microstructure and Texture Evolution of Magnesium alloy after Shear Assisted Processing and Extrusion (ShAPE TM), in: 18th Int. Conf. Textures Mater., 2018. doi:10.1088/1757-899X/375/1/012007.

29. S. Whalen, V. Joshi, N. Overman, D. Caldwell, C. Lavender, T. Skszek, Scaled-Up Fabrication of Thin-Walled ZK60 Tubing Using Shear Assisted Processing and Extrusion (ShAPE), in: *Magnes. Technol.* 2017, 2017. doi:10.1007/978-3-319-52392-7.

30. I.J. Beyerlein, R.J. McCabe, C.N. Tomé, Effect of microstructure on the nucleation of deformation twins in polycrystalline high-purity magnesium: A multi-scale modeling study, *J. Mech. Phys. Solids.* 59 (2011) 988–1003. doi:10.1016/j.jmps.2011.02.007.

31. X.L. Wu, K.M. Youssef, C.C. Koch, S.N. Mathaudhu, L.J. Kecskés, Y.T. Zhu, Deformation twinning in a nanocrystalline hcp Mg alloy, *Scr. Mater.* 64 (2011) 213–216. doi:10.1016/j.scriptamat.2010.10.024.

32. D. Yi, W. Gu, X. Fang, B. Wang, W. Luo, Plastic deformation behaviors and dynamic recrystallization mechanisms of ZK60 magnesium alloy, *Int. J. Soc. Mater. Eng. Resour.* 14 (2006) 33–39. doi:10.5188/ijssmer.14.33.

33. X. Gong, W. Gong, S. Bong, J. Hyung, Effect of Warm Rolling on Microstructure and Mechanical Properties of Twin-roll Casted ZK60 Alloy Sheets, *Mater. Res.* 18 (2015) 360–364. doi:10.1590/1516-1439.319314.

34. W. Jin, J. Fan, H. Zhang, Y. Liu, H. Dong, B. Xu, Microstructure, mechanical properties and static recrystallization behavior of the rolled ZK60 magnesium alloy sheets processed by electropulsing treatment, *J. Alloys Compd.* 646 (2015) 1–9. doi:10.1016/j.jallcom.2015.04.196.

Pacific Northwest National Laboratory

902 Battelle Boulevard
P.O. Box 999
Richland, WA 99354
1-888-375-PNNL (7665)

www.pnnl.gov